

New method to find operating points for multi-PID control. Application to vehicle lateral guidance.

Nolwenn Monot ^{*,**,***} Xavier Moreau ^{**,***}
André Benine-Neto ^{**,***} Audrey Rizzo ^{*,***}
François Aioun ^{*,***}

^{*} PSA Group, 78943 Vélizy-Villacoublay, France (e-mail: *firstname.lastname@mps.com*).

^{**} Laboratory IMS, UMR 5218 CNRS, University of Bordeaux, 33405 Talence, France (e-mail: *firstname.lastname@ims-bordeaux.fr*)

^{***} OpenLab PSA Group and IMS Laboratory ^{*}

Abstract: This paper proposes a new approach to find operating points for gain scheduling control using PID controllers. The operating point are computed with a frequency analysis of the system that gives the number of operating points needed and their values. The PID are weighted in their operating area using continuous functions that depend on the scheduling parameter. A concrete example of an autonomous vehicle lateral guidance shows the effectiveness of the method comparing different configuration of operating points and weights.

Keywords: PID control, Control system design, Time varying systems, Time scheduling control, Dynamics.

1. INTRODUCTION

The PID is a renown controller, often used in industry for its design simplicity and its efficiency for most of the systems.

The problem of a classic PID is that the parameters are fixed but the system to control may have varying parameters. These varying parameters may cause a loss of performances of the closed-loop, or the instability of the system. Several solutions have been developed like the adaptive PID in Mahapatra et al. (2016) and Kuc and Han (2000). This solution changes the parameters of the PID in function of the measured output. There also exist approaches that use neural network to compute the parameters of the PID like in Shu and Guo (2004). Another way to resolve the problem of varying parameters is to use fuzzy logic theory. Many researches investigated this solution using PID controller like in Khan and Rapal (2006) or Jantzen (1998). The idea is to compute PID like actions using fuzzy inference.

The other important theory of control for time varying system is the gain scheduling control theory. This theory uses scheduling variables that have a significant impact on the system dynamics. Several PID for different operating points depending on the scheduling variables are computed. The controller used for the regulation is the PID with the operating point closest to the actual value of the scheduling variables or an interpolation between PIDs.

An overview of the methods has been written in Leith and Leithead (2000).

The main problems of the gain-scheduled theory is to chose the operating points where the system is linearized to compute the PIDs and how to combine the controllers. In most of the researches as in De Oliveira and Karimi (2012), operating points are chosen manually, there is however a method named gap metric emerging like in Tan et al. (2004) enabling to calculate the operating points. As stated in Du and Johansen (2014) the two methods to interpolate the PIDs are: switches between the controllers or weights with Gaussian functions, trapezoidal functions or Bayesian functions.

The weighted multi-PID presented here is a gain scheduled controller using several PID. The contribution of each PID is based on weights that depend on an activation parameter. These weights are continuous sigmoid functions and the activation parameter is a measurable parameter of the system that vary though time. In order to use a multi-PID, this parameter should have a significant impact on the system dynamics such that the robustness or the stability to this parameter variation are not granted.

The method for multi-PID control introduced here enables, by an analysis of the system dynamics in the frequency domain, to easily find the operating points.

An example is provided with the lateral guidance of an autonomous vehicle. The paper shows that the longitudinal speed influences significantly the lateral dynamics of the vehicle. Thus, this parameter is used as the activation parameter for the design of the multi-PID.

^{*} This work took place in the framework of the OpenLab 'Electronics and Systems for Automotive' combining IMS laboratory and Groupe PSA company.

The paper is organized as follows. section 2 presents the methodology developed for the design of gain-scheduling with PID controllers and section 3 provides an example of the previous solution with several configuration of the controllers using the application case of autonomous vehicle lateral guidance. Section 4 wraps up the paper with conclusions and perspectives.

2. METHODOLOGY

2.1 Design of a PID

When the equations that determine the system dynamics are known, it is easier and faster to tune the PID parameters using the equations in the frequency domain to obtain the desired performances. These performances are expressed with several parameters used for the design of the PID. This parameters are:

- the open-loop crossover frequency ω_u : reflects the system rising time,
- the phase margin M_ϕ : reflects the stability of the closed loop.

These parameters are usually defined by the specification of the system.

A PID has the form:

$$C(s) = C_0 \left(\frac{1 + s/\omega_i}{s/\omega_i} \right) \left(\frac{1 + s/\omega_1}{1 + s/\omega_2} \right), \quad (1)$$

where C_0 is a proportional gain, ω_i such that $\omega_i = \omega_u/10$ is the transitional frequency, ω_1 and ω_2 are the cutoff frequencies of the lead or lag compensator.

Knowing that the open-loop transfer of a system $G(s)$ and a controller $C(s)$ function is written:

$$\beta(j\omega) = C(j\omega)G(j\omega), \quad (2)$$

the frequencies ω_1 and ω_2 are obtained in the respect of the desired phase margin:

$$M_\phi = \arg(\beta(j\omega_u)) + \pi, \quad (3)$$

with

$$\begin{aligned} \arg(\beta(j\omega_u)) &= \arg(C(j\omega_u)G(j\omega_u)) \\ &= \arg(C(j\omega_u)) + \arg(G(j\omega_u)). \end{aligned} \quad (4)$$

The gain C_0 is computed with the equation:

$$|\beta(j\omega_u)| = |C(j\omega_u)G(j\omega_u)| = 1. \quad (5)$$

2.2 Design of a weighted multi-PID: choice of the weights and the operating points

However, when the system to control is more complex and its dynamics can change through time, a PID alone may not be able to guarantee the desired performances and respect the specifications.

Several PID controllers are computed for different operating points. There is not a clear method to chose the operating points in multi-control research. In most cases, these points are chosen manually

The system to regulate has the steady-state space representation:

$$\begin{cases} \dot{x}(t) = A(\xi(t))x(t) + B(\xi(t))u(t) \\ y(t) = Cx(t), \end{cases} \quad (6)$$

$x(t)$ is the state vector, $u(t)$ the input control, $y(t)$ the output and $A(\xi(t))$, $B(\xi(t))$, C are the state space matrices. These two first matrices depend on a variable parameter $\xi(t)$ leading to a time varying system.

The parameter ξ can vary on an interval $[\xi_{min}, \xi_{max}]$. The objective of the multi-PID controller is to control the system on all this interval range. ξ is thus used to chose the operating points and as the activation parameter for the weights of the PIDs.

The difficulty in the chose of the operating points is to determine:

- N_{op} : the number of operating points,
- ξ_i : the values of the variable parameter of the operating points, with $i \in \mathbb{N}$ such that $i \in [1, N_{op}]$.

An intuitive way to chose ξ_i would be to divide the interval $[\xi_{min}, \xi_{max}]$ into $N_{op} - 1$ equal parts such that $\forall i \in [1, N_{op} - 1]$:

$$\xi_{i+1} - \xi_i = \text{Var}_\xi, \quad (7)$$

with Var_ξ is the variation of ξ between two operating points.

However, ξ may not have a linear influence on the system dynamics and this method does not give N_{op} that still needs to be chosen manually.

To find the operating points, the method developed here uses the phase variation of the plant at the crossover frequency in function of ξ . N_{op} and ξ_i are chosen so that between two consecutive operating points ξ_i the phase variation of the plant between two operating points is Var_ϕ :

$$\left| \arg(G(j\omega_u)|_{\xi_{i+1}}) - \arg(G(j\omega_u)|_{\xi_i}) \right| = \text{Var}_\phi \quad (8)$$

The parametrization of Var_ϕ instead of N_{op} and Var_ξ enables to find an optimal number of operating points with an optimal distribution. Var_ξ is chosen as the result of a trade-off between robustness, performance and number of sub-systems. An empiric value of Var_ξ could be $\text{Var}_\xi = 15^\circ$.

Once ξ_i are identified, the system is linearized around these operating points and the associated PID is computed using (1) - (5).

As stated previously, each PID is activated using weights. In order to keep the continuity at ξ_i , sigmoid functions are used as the weighs of the PIDs. A sigmoid $f_\lambda(x)$, with $x \in \mathbb{R}$, $\lambda \in \mathbb{R}$, is written:

$$f_\lambda(x) = \frac{1}{1 + e^{-\lambda x}}. \quad (9)$$

The weights w_i of the PID corresponding to the operating point ξ_i is calculated with the relation:

$$w_i(\xi) = 1 - f_{\lambda_i}(\xi) + f_{\lambda_{i-1}}(\xi), \quad (10)$$

with $1 - f_{\lambda_i}(\xi)$ the sigmoid on the interval $[\xi_i; \xi_i + 1]$ and $f_{\lambda_{i-1}}(\xi)$ the sigmoid on the interval $[\xi_{i-1}; \xi_i]$.

The weighted multi-controller can be written:

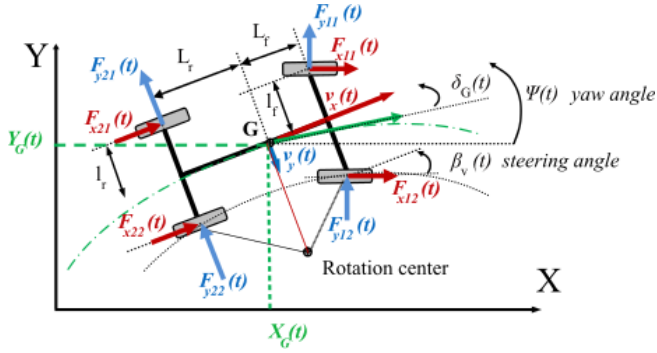


Fig. 1. Forces scheme

$$PID(s) = \sum_{i=1}^{N_{op}} w_i(\xi) PID_i(s), \quad (11)$$

3. APPLICATION TO VEHICLE LATERAL GUIDANCE

This section provides a concrete example for the design of a weighted PID and showing the influence of the parameters Var_ϕ , N_{op} and Var_ξ used in section 2 for the design of the controller. The example treats the case of a vehicle lateral guidance in the context of an autonomous vehicle. The objective is to regulate the vehicle lateral position using a steering wheel control. There is no human interaction and the vehicle should be able to follow the desired trajectory at all speeds, which is used as the activation parameter such that $\xi(t) = V_x(t)$.

3.1 Four wheels vehicle model

The vehicle is modelled using a four wheel model. In this example, the masses on the right and left wheelbases are considered equal such that the four wheel model can be assimilated to a bicycle model. The equations linked to the model and the linearization are explained in Monot et al. (2017).

The state-space representation is defined using the signals of yaw rate ($\dot{\psi}(t)$), yaw ($\psi(t)$), transverse speed ($v_y(t)$), lateral position ($y_G(t)$) and steering-wheel angle ($\theta_v(t)$):

$$\begin{cases} \dot{\underline{x}}(t) = A\underline{x}(t) + Bu(t) \\ y(t) = C\underline{x}(t), \end{cases} \quad (12)$$

with the state vector $\underline{x}(t) = (\psi(t) \dot{\psi}(t) v_y(t) y_G(t))^T$, the input control $u(t) = \theta_v(t)$ and the output $y(t) = y_G(t)$.

All this signals can be seen on the vehicule scheme with Fig. 1.

The matrices of the state-space representation (12) are:

$$A = \begin{bmatrix} 0 & 1 & 0 & 0 \\ 0 & -\frac{2(L_f^2 c_{yf} + L_r^2 c_{yr})}{I_z V_{x0}} & -\frac{2PDE}{I_z V_{x0}} & 0 \\ 0 & -\frac{2PDE}{M_t V_{x0}} - V_{x0} & -\frac{2(c_{yf} + c_{yr})}{M_t V_{x0}} & 0 \\ V_{x0} & 0 & 1 & 0 \end{bmatrix}, \quad (13)$$

$$B = \begin{bmatrix} 0 & \frac{2c_{yf}L_f}{\lambda I_z} & \frac{2c_{yf}}{\lambda M_t} & 0 \end{bmatrix}^T \quad (14)$$

and

$$C = [0 \ 0 \ 0 \ 1], \quad (15)$$

with $PDE = L_f c_{yf} - L_r c_{yr}$. All the parameters of the model are described in Table 1.

Table 1. Parameters of the dynamic system

V_{x0}	Longitudinal speed	Between 1 km/h and 130 km/h
μ	Road adhesion	1
M_t	Total mass of the vehicle	1759 kg
$M_{f/r}$	Front / rear mass	1319 kg / 439 kg
I_z	Moment of inertia	2638 kg.m ²
$L_{f/r}$	Front / rear wheelbase	0.71 m / 2.13 m
$c_{yf/r}$	Front / rear transverse cornering stiffness	94446 N.rad ⁻¹ / 48699 N.rad ⁻¹
λ	Steering column gear rate	16

3.2 Frequency analysis

The transfer function needed for the design of the controller is $G(s) = \frac{Y_G(s)}{\Theta_v(s)}$. It is calculated using the relation:

$$G(s) = \frac{Y_G(s)}{\Theta_v(s)} = C[sI - A]^{-1}B. \quad (16)$$

It gives:

$$G(s) = \frac{K_0}{s^2} \frac{1 + 2\zeta_1(s/\omega_1) + (s/\omega_1)^2}{1 + 2\zeta_0(s/\omega_0) + (s/\omega_0)^2}, \quad (17)$$

where ζ_0 , ζ_1 , ω_0 , ω_1 and K_0 can be expressed according to the vehicle parameters, the road adhesion and the longitudinal speed such that:

$$\begin{aligned} K_0 &= \frac{2c_{yf}c_{yr}V_{x0}^2L}{\lambda(2c_{yf}c_{yr}L^2 - M_tV_{x0}^2PDE)}, \\ \zeta_0 &= \frac{M_t(L_f^2c_{yf} + L_r^2c_{yr}) + I_z(c_{yf} + c_{yr})}{\sqrt{2I_zM_t(2c_{yf}c_{yr}L^2 - M_tV_{x0}^2PDE)}}, \\ \omega_0 &= \sqrt{2} \sqrt{\frac{2c_{yf}c_{yr}L^2 - M_tV_{x0}^2PDE}{I_zM_tV_{x0}^2}}, \\ \zeta_1 &= \frac{L_f}{V_{x0}} \sqrt{\frac{c_{yr}L}{2I_z}}, \\ \omega_1 &= \sqrt{2} \frac{c_{yr}L}{I_z}, \end{aligned} \quad (18)$$

with $L = L_f + L_r$.

In this application, the road is assumed to be dry and the mass of the vehicle is supposed to be fixed. The objective is to regulate the vehicle transverse position at all speed. So as to assess the influence of the vehicle longitudinal speed on the vehicle lateral dynamics, the transfer function $G(s)$ is plotted in frequency domain on Fig. 2 with different V_{x0} .

An important variation of the dynamic can be observed. There is an inversion between the poles and zeros that leads the system to be a natural phase lead at low speeds and phase lag at high speeds.

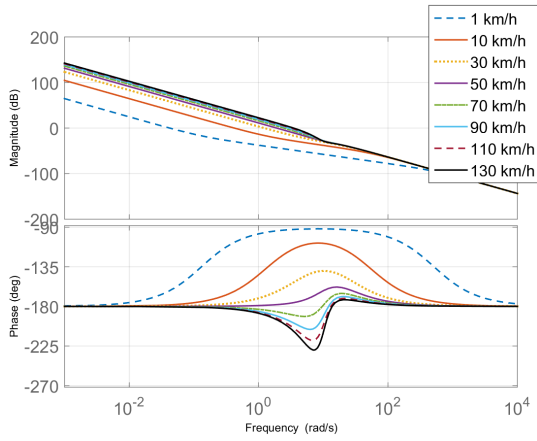


Fig. 2. Bode diagram of $G(s)$

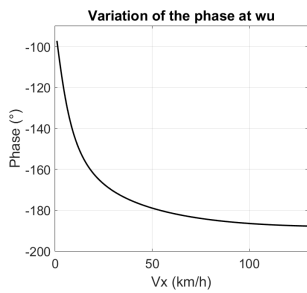


Fig. 3. Phase variation of $G(s)$ at ω_u

With this figure, it is easy to assume that a PID alone cannot guaranty the stability of the system at all speeds. The method of weighted multi-PID described above will be applied in the following subsections.

3.3 Specifications

To design the PIDs of the multi-controller, the open-loop crossover frequency ω_u and the phase margin M_Φ described in section 2.2 need to be defined.

For this application, in order to respect the human behavior, the open-loop crossover is chosen to respect human behavior such that $\omega_u = 1\text{rad/s}$. As for the phase margin, it is chosen as the empiric value $M_\Phi = 45^\circ$.

At $\omega_u = 1\text{rad/s}$, the phase of the plant $G(s)$ does not vary linearly as it can be seen from Fig. 3.

This variation will have a huge impact on the open-loop in function of the controller.

3.4 Frequency comparison of weighted multi-PID controllers using different parameters for the design

In this section, several multi-controllers are compared using different values for the parameters Var_ξ , Var_ϕ and N_{op} . Table 2 summarizes the 6 different parametrization.

For 3 different N_{op} (3, 4 and 7), the intervals with Var_ξ and Var_ϕ are compared. It can be noticed that for a same number of operating points, the intervals with constant ξ variation and the intervals with constant phase variation do not lead to the same operating points.

Table 2. Parameters of the dynamic system

	$\text{Var}_{\phi/\xi}$	N_{op}	ξ_i (km/h)
Var_ξ	64.5 km/h	3	1/65/130
	43 km/h	4	1/44/87/130
	21.5 km/h	7	1/22.5/44/65.5/87/108.5/130
Var_ϕ	45°	3	1/9.6/130
	30°	4	1/5.8/16.7/130
	15°	7	1/3.2/5.9/9.8/17/35.4/130

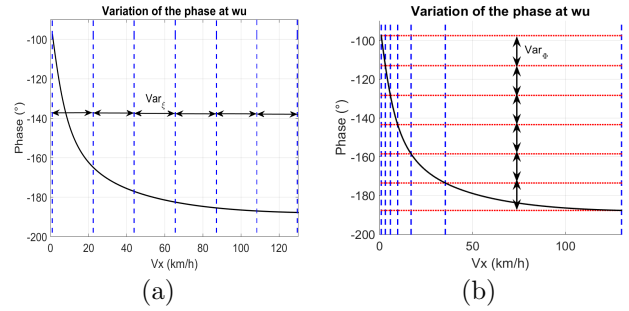


Fig. 4. Cutting used for the chose of the speeds operating point with Var_ξ constant (a) and Var_ϕ constant (b)

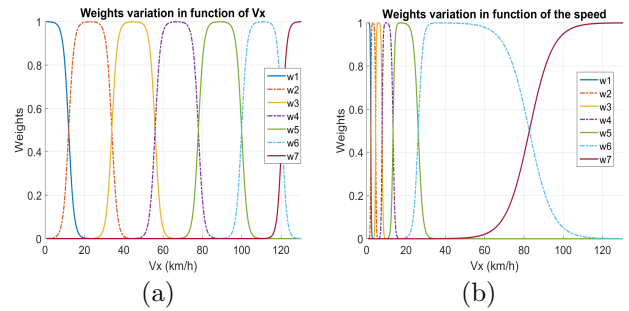


Fig. 5. Examples of weights for multi-controller with 7 PID and cutting with Var_ξ constant (a) and Var_ϕ constant (b)

Since $G(j\omega_u)$ presents more phase variation for low speed than for high speed, the proposed method based on intervals of Var_ϕ results in more operating points for low speeds. The intervals for the examples of $\text{Var}_\phi = 15^\circ$, leading to $N_{op} = 7$ and $\text{Var}_\xi = 21.5$ km/h can be observed on Fig.4.

The computation of the operating points has an impact on the weights. For the same example of $N_{op} = 7$, the weights are plotted on Fig.7.

For a closed loop-system, the stability can be analyzed using the Bode stability criterion: a closed-loop system is stable if the phase margin of the open-loop is superior to 0, $M_\Phi > 0$. This criterion can only be applied to minimum phase systems, meaning that the poles and zeros of the system $G(s)$ are in the left half of the complex plan. In this example, $G(s)$ is a minimum phase system so the Bode stability criterion can be used (Shinners (1998)).

In order to verify that the stability of the closed-loop is guarantee at all speeds, the phase margin M_ϕ of the open-loop for the different controller configurations of Table 2 are plotted on Fig. 6 in function of the speed. It can be

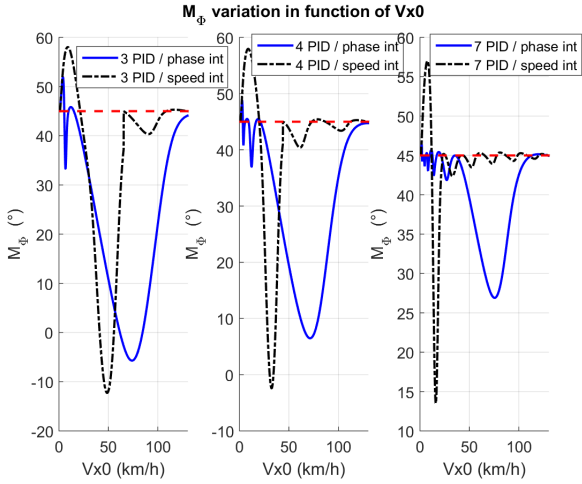


Fig. 6. Phase margin M_Φ of the open-loop for the different combinations

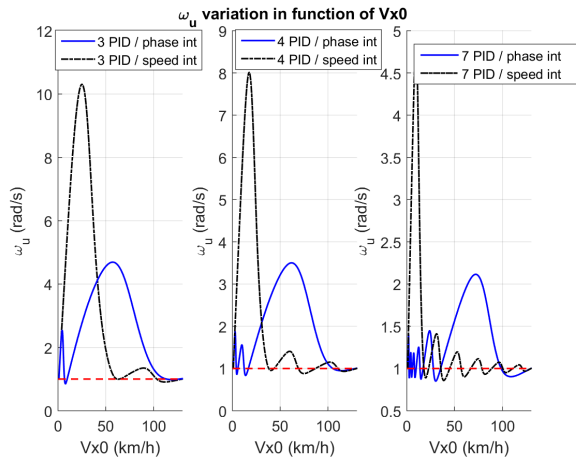


Fig. 7. ω_u of the open-loop for the different combinations

seen that 3 operating points is not enough to keep the system stable at all speed for both configurations with Var_ξ constant and Var_ϕ constant. With 4 operating points chose with Var_ϕ constant, the phase margin stay positive at all speeds whereas the configuration with Var_ξ constant is still unable to ensure stability at low speed. This is due to the system high sensibility to speed variation and the suboptimal positioning of the ξ_i operating points. 7 operating points is sufficient for both solution to keep the closed-loop stable. The multi-controller designed with constant Var_ϕ shows a better degree of stability at low speeds than the multi-controller designed with constant Var_ξ while it is the reverse at high speeds. However, the multi-controller designed with constant Var_ξ has higher peak of M_Φ at low speed, so a lower stability degree, because of the lack of controllers in this range of speed.

In term of open-loop crossover frequency, as for the phase margin, the multi-controller with constant Var_ξ has higher peak at low speed where there is a lack of operating points but it stays close to the desired value at high speed because there is an oversampling of operating points.

The open-loop frequency responses are plotted in Nichols chart on Fig. 8-13 for the system linearized at several speeds: 1, 10, 30, 50, 70, 90, 110, 130 km/h. Even if all

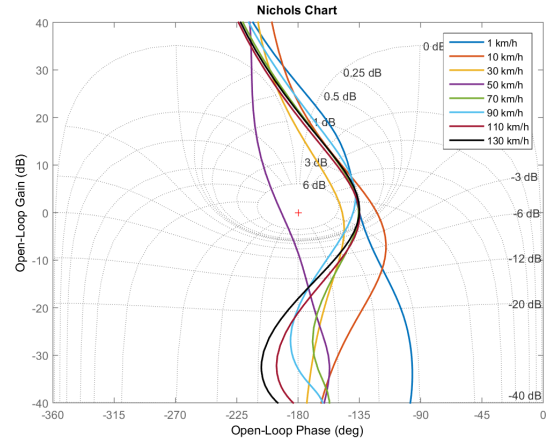


Fig. 8. Open-loop Nichols chart with Var_ξ constant for $N_{op} = 3$

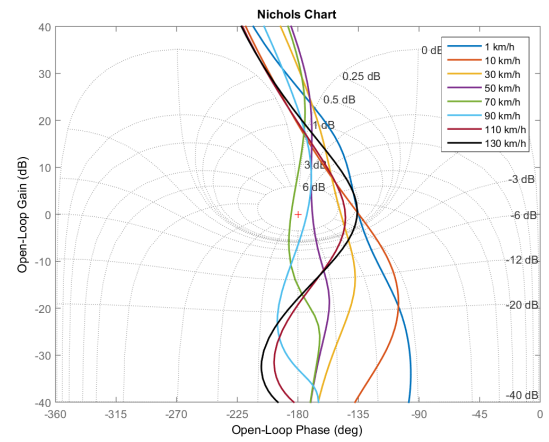


Fig. 9. Open-loop Nichols chart with Var_ϕ constant for $N_{op} = 3$

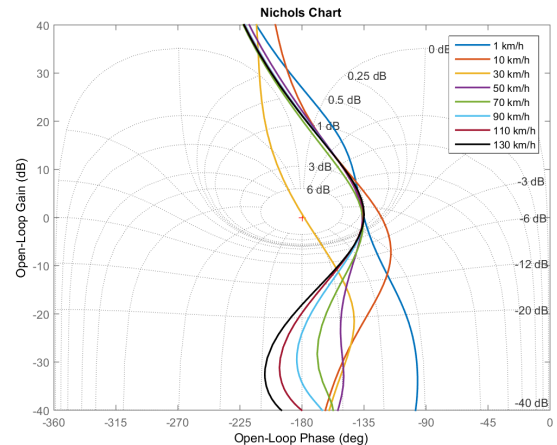


Fig. 10. Open-loop Nichols chart with Var_ξ constant for $N_{op} = 4$

the possibility of the open-loop configurations for different longitudinal speeds are not plotted due to readability problem, it can be observed that the closed-loop is not robust to speed variation when $N_{op} = 3$ and $N_{op} = 4$. Indeed, when $N_{op} = 3$, on Fig. 8 and Fig. 9, the instability problem can be seen for several speeds. When $N_{op} = 4$, it can be seen that there is a high sensibility around 30km/h

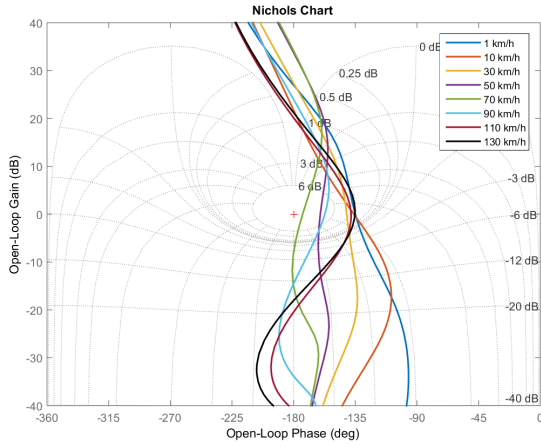


Fig. 11. Open-loop Nichols chart with Var_ϕ constant for $N_{op} = 4$

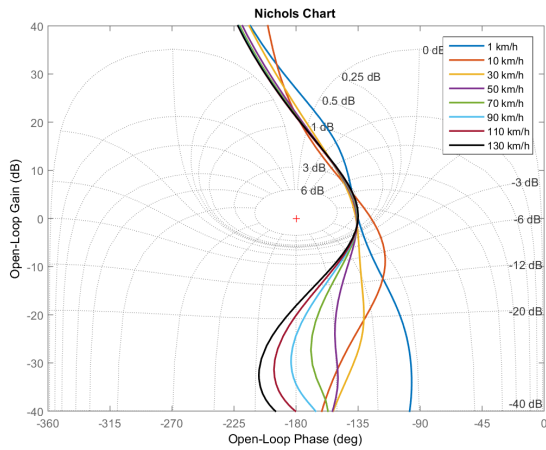


Fig. 12. Open-loop Nichols chart with Var_ξ constant for $N_{op} = 7$

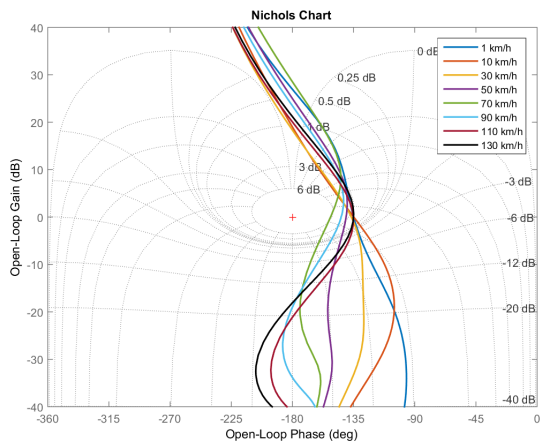


Fig. 13. Open-loop Nichols chart with Var_ϕ constant for $N_{op} = 7$

for the multi-controller with Var_ξ constant on Fig. 10 and that for Var_ϕ constant on Fig. 11 the Q-factor varies significantly at high speed. For $N_{op} = 7$, on Fig. 12 and Fig. 13, a robustness of the stability degree can be observed for both configurations with the plotted curves.

4. CONCLUSION

In this paper, a new method to simply and efficiently chose operating points for gain-scheduling control has been presented. It has been showed that it is more reasonable to position the operating points with a constant phase variation at the desired open-loop crossover frequency instead of using a fixed variation of the time varying parameter. The continuity of the closed-loop is guaranteed using continuous weights.

The efficiency of the proposed method has been shown in the context of lateral guidance of autonomous vehicles, in which the longitudinal velocity varies from 1 to 130km/h. Further work will deal with the extension of the method to systems with more than 1 variable parameter. Also, this method can only be used for measured parameter and the PID is not robust to uncertain parameters. So this method will be expand with robust controllers instead of PID in order to make a gain-scheduling control robust to uncertain parameters.

REFERENCES

- De Oliveira, V. and Karimi, A. (2012). Robust and gain-scheduled pid controller design for condensing boilers by linear programming. *IFAC Proceedings Volumes*, 45(3), 335–340.
- Du, J. and Johansen, T.A. (2014). A gap metric based weighting method for multimodel predictive control of mimo nonlinear systems. *Journal of Process Control*, 24(9), 1346–1357.
- Jantzen, J. (1998). Tuning of fuzzy pid controllers. *Technical University of Denmark, Department of Automation, Bldg*, 326.
- Khan, A.A. and Rapal, N. (2006). Fuzzy pid controller: design, tuning and comparison with conventional pid controller. In *Engineering of Intelligent Systems, 2006 IEEE International Conference on*, 1–6. IEEE.
- Kuc, T.Y. and Han, W.G. (2000). An adaptive pid learning control of robot manipulators. *Automatica*, 36(5), 717–725.
- Leith, D.J. and Leithead, W.E. (2000). Survey of gain-scheduling analysis and design. *International journal of control*, 73(11), 1001–1025.
- Mahapatra, S.D., Saha, R., Sanyal, D., Sengupta, A., and Bhattacharyya, U. (2016). Adaptive pid control for angular motion tracking by linear electrohydraulic actuation. In *Power Electronics, Intelligent Control and Energy Systems (ICPEICES), IEEE International Conference on*, 1–5. IEEE.
- Monot, N., Moreau, X., Benine-Neto, A., Rizzo, A., and Aioun, F. (2017). Dynamic stability control system: the crone approach. *IFAC-PapersOnLine*, 50(1), 13822–13827.
- Shinners, S.M. (1998). *Modern control system theory and design*. John Wiley & Sons.
- Shu, H. and Guo, X. (2004). Decoupling control of multivariable time-varying systems based on pid neural network. In *Control Conference, 2004. 5th Asian*, volume 1, 682–685. IEEE.
- Tan, W., Marquez, H.J., and Chen, T. (2004). Operating point selection in multimodel controller design. In *American Control Conference, 2004. Proceedings of the 2004*, volume 4, 3652–3657. IEEE.